Contribution to the validation of the MORET 5 code using the CROCUS reactor physics benchmark

Nicolas Leclaire, Bertrand Cochet

Contribution to the verification of the MORET 5 code using the CROCUS reactor physics benchmark

N. Leclaire[a*], B. Cochet[a**]

[a]*Institut de Radioprotection et de Sûreté Nucléaire (IRSN), PSN-RES, SNC, LN, Fontenay-Aux-Roses, 92262, France*

ABSTRACT

The present paper focuses on the modeling of the CROCUS reactor with the French MORET 5 continuous energy code and compares k_{eff}, anti-reactivity effects (variation of k_{eff} normalized to k_{eff} due to the insertion of an absorber), sensitivity coefficients and kinetics parameters with those provided by other reference codes. The aim is mainly to extend the experimental validation/verification database of the MORET 5 code to use reactor physics applications. A suite of about 1400 benchmarks is already available for criticality but only a few are dedicated to reactor physics applications. The CROCUS reactor configurations therefore constitute an opportunity to test and improve the implementation of kinetics parameters and sensitivity coefficients in the code and make a verification of these physical quantities through the comparison with other codes such as MCNP. Moreover, it has offers the opportunity to quantify the effect of nuclear data processing through the use of two different data processing codes.

KEYWORDS:
Absorber rods
Verification
CROCUS
Kinetics parameters
Light water reactor
Reactivity effects

[*]Corresponding Author,
E-Mail address: nicolas.leclaire@irsn.fr (N. Leclaire)
** *Now Commissariat à l'Energie Atomique et aux énergies alternatives*

1. Introduction

The MORET 5 (Cochet et al., 2015) Monte Carlo code developed since 2008 at IRSN targets criticality-safety applications. It has been first involved in an industrial calculation route within the CRISTAL package (Gomit et al., 2017) coupled with the deterministic APOLLO2 code (Sanchez et al., 2010) for the calculation of k_{eff}. Then, a continuous energy version was developed outside the CRISTAL package. Up to now four versions of this continuous energy code have been released, the last one being MORET 5.D.1, incorporating developments such as:

- probability tables to describe cross sections in the unresolved energy range,
- nuclear data sensitivity based on the Iterated Fission Probability methodology (IFP) (Kiedrowski et al., 2013) allowing, among other possibilities, calculation of nuclear data biases through the use of sensitivity/uncertainty analyses using GLLSM (Jinaphanh et al., 2017 and Leal et al., 2019),
- reaction rates calculations for reactor physics,
- a new model for kinetics parameters calculations based on a new estimate of the adjoint flux and therefore improving the existing one that did not follow the population of fission neutrons over more than one generation (Jinaphanh et al., 2010).

One of the evolutions of the MORET 5 code deals with reactor physics applications. Thus a more complex capability to better model the calculation of kinetics parameters has been recently developed in the MORET 5.D.1 code. That is also the reason why IRSN extended its experimental validation/verification database already composed of more than 1400 experimental cases in order to cover such applications, using benchmarks from the IRPhe (NEA/NSC/DOC(95)03, 2017) Handbook.

The aim of the paper is to test and validate the use of the MORET 5 code for reactor physics applications comparing the values obtained for reactivity effects, kinetics parameters according with the new code implementation, sensitivity to nuclear data with the ones obtained with other codes such as the MCNP6 code (F. Brown et al., 2017).

The CROCUS reactor offers the opportunity to test in particular the calculation of reactivity values and kinetics parameters. Indeed, in this program, three kinds of experiments are proposed (IRPhe Handbook):

- an exactly critical experiment, without absorber rods, for which criticality is reached by varying the water level in the reactor;
- slightly over critical experiments, without absorber rods, for which the level of water was raised until delayed critical;
- slightly over critical experiments, with absorber rods; in that case, an absorber rod (boron or erbium) was introduced in the core and the level of water was adjusted to be critical; then the reactor was made supercritical by removing the absorber rod and keeping the water level constant.

Comparisons are made mainly on reactivity values with the Monte Carlo MCNP5 and MCNP6 codes using the ENDF/B-VII.0 evaluation for nuclear data, as well as with TRIPOLI results (Zoia et al., 2016) using also a library based on the same evaluation. The results using the data processed by MCNP are compared with those using data processed with the homemade GAIA processing tool (Haeck et al., 2015). The objective is to validate the physical models implemented in the MORET 5 code and identify potential processing issues. Moreover, libraries based on various evaluations and processed identically are tested for the MORET 5 code just to assess the impact of the evaluation on the results.

Concerning the kinetics parameters, only global quantities, without distinguishing by precursor group, are estimated by the MORET 5 code. As a result, the effective delayed neutron fraction cannot be estimated by group of precursor.

In section 2, we describe the CROCUS reactor configuration.

Section 3 discusses the codes and libraries used for the calculations.

In section 4, one gives the definition of kinetics parameters.

In section 5, the methodology of verification is described.

Section 6 focusses on the results before concluding in section 7.

2. Description of the experiments

The CROCUS reactor, operated by the Swiss Federal Institute of Technology (EPFL), Lausanne, is a zero power reactor, with a maximum allowed power of 100 W. It is constituted of a two-zone uranium-fueled, H_2O-moderated critical core. This core is approximately cylindrical in shape with a diameter of about 60 cm and a height of 100 cm. In 1995, in the CROCUS reactor a configuration with a central zone of 1.806 wt.%-enriched UO_2 rods and an outer zone of 0.947 wt.%-enriched uranium metal rods was made critical by raising the water level. The description is issued from the IRPhe Handbook.

Six experiments are described and are considered to be of benchmark quality (IRPhe Handbook). Experiment 1 does not involve any absorbing rod; it is critical (inverse

period equal to zero). Experiments 2 to 4 do not involve any absorbing rod but are slightly supercritical[b]. Experiments 5 and 6 involve either boron in an absorbing rod or erbium. They are also slightly supercritical. They are provided in Table 1.

Table 1
Benchmarks cases heights and inverse periods (IRPhe Handbook).

Case Number	Absorber Material	Case Name	Water level (cm)	Inverse Period ω (sec^{-1})
1	No absorber	$H_1 = H_{crit}$	96.51	0.0
2		H_2	98.51	1.3422E-02
3		H_3	99.00	1.8180E-02
4		H_4	99.51	2.3392E-02
5	Soluble Boron	Boron	96.92	1.2856E-02
6	Erbium	Erbium	98.63	3.2976E-02

2.1. Geometry

The core is made of two lattices of rods in water (see Fig. 1 and Fig. 2):

- a central lattice of 336 U(1.806 wt.%)O_2 rods with aluminum clads at a 1.837-cm square pitch;
- a driver array of 172 (176 if absorber rods) metallic uranium rods with a 0.947 wt.% enrichment in ^{235}U with aluminum clads at a 2.917-cm square pitch.

The characteristics of rods are provided in Table 2.

At the center, the core can accommodate two absorbing rods introduced in the core one at a time. The first rod clad with aluminum was filled with borated water (6768 ppm natural boron). The second one with aluminum clads contained pellets with 3.72 g/cm^3 ZrO_2 and 0.874 g/cm^3 Er_2O_3.

Criticality is reached increasing the water level; the reactor can be slightly supercritical. The measurement of the inverse period ω_1 of the in-hour equation allows determining the critical state. This quantity can be easily approximated using formula (1):

$$Ln\left(\frac{P(t)}{P(0)}\right) = \omega_1 t \qquad (1)$$

P(t) being the power of the reactor at time t.

Table 2
Main characteristics of rods (**IRPhe Handbook**).

Parameter	UO_2	U_{metal}
Cladding Thickness (mm)	0.85	0.975
External cladding diameter (mm)	12.6	19.3
Fuel diameter (mm)	10.52	17.0
Square pitch (mm)	18.370	29.17

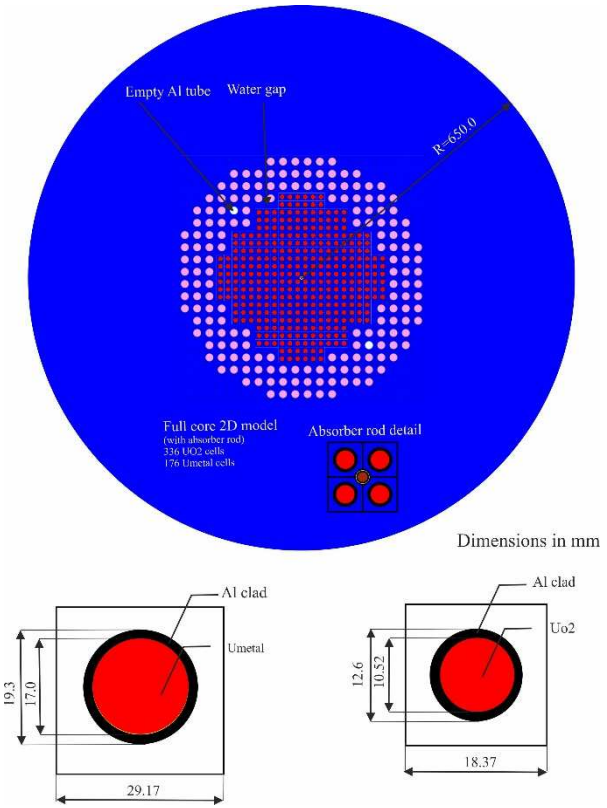

Fig. 1. Cross section view from above of CROCUS reactor.

The slowing down density calculated by the MORET 5.D.1 Monte Carlo code,

[b] It means that k_{eff} does not exceed a few hundreds of pcm.

corresponding to the proportion of neutrons that undergo fissions below 4 eV, is equal to 0.8138, proving that the neutron spectrum of the configuration is thermal.

2.2. Chemical media

2.2.1 UO_2 rods

The UO_2 fuel rods of the internal zone had a ^{235}U enrichment of 1.806 wt. %. They were immersed in light water. A description of the UO_2 rods is given in Fig. 3.

The density of the fuel pellets was 10.556 g/cm^3.

2.2.2 U_{metal} rods

The U_{metal} rods of the peripheral zone had a ^{235}U enrichment of 0.947 wt. %. They were immersed in light water. The density of the fuel pellets was 18.677 g/cm^3. A description of the rods is given in Fig. 4.

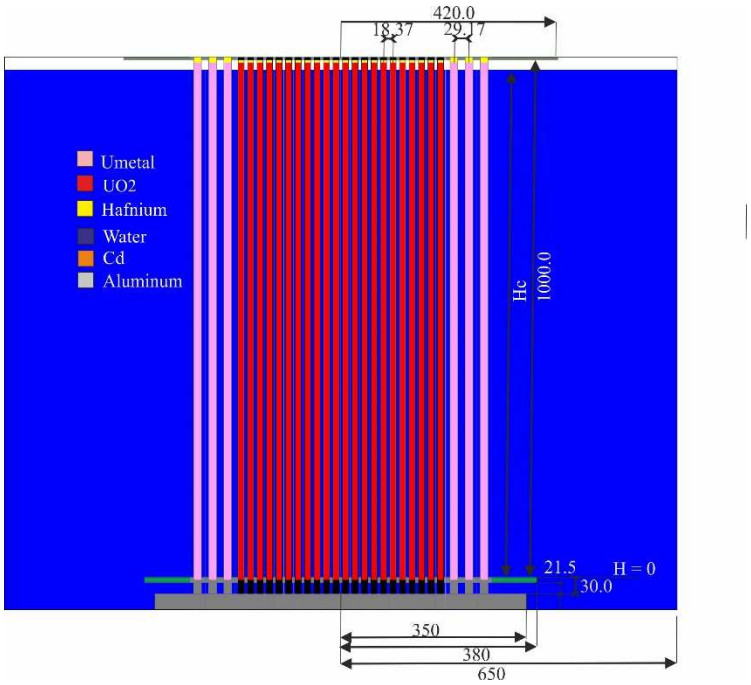

Fig. 2. Lateral view of CROCUS reactor.

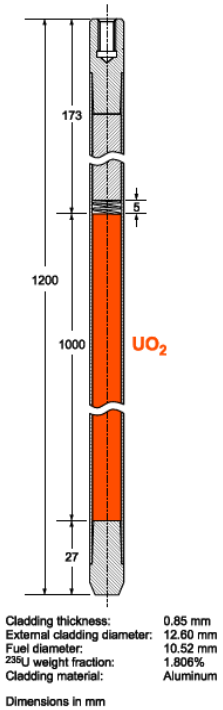

Fig. 3. UO_2 fuel rods (courtesy of the IRPhe).

2.3. Critical approach

The critical configuration containing 172 metallic U fuel rods (176 if absorber rods) was made critical by adjusting the water level. The water level was then raised up, the reactor becoming supercritical. After some time (30-40 sec) in order to allow for the transients to vanish, the flux increased exponentially. The time variation of the flux curve was measured with a multichannel analyser (IRPhe Handbook), and the inverse reactor period was determined from the slope of the flux curve. One critical configuration (denoted H1), where the inverse reactor period is zero, and 3 supercritical ones were measured in that way.

For the configurations involving an absorber rod (Boron or Erbium), the number of metallic U fuel rods was slightly different (176 instead of 172). The absorber rod containing either borated water or Zirconium-Erbium pellets was located at the very centre of the configuration, between the four central UO_2 rods. With the absorber rod inserted, the reactor was made critical by adjusting the water level. Afterwards, the absorber rod was withdrawn, the water level being kept constant. Therefore, the reactor became supercritical, and the slope of the flux curve was measured. Two critical configurations with an absorber rod inserted and two supercritical configurations after withdrawing the absorber rod were measured.

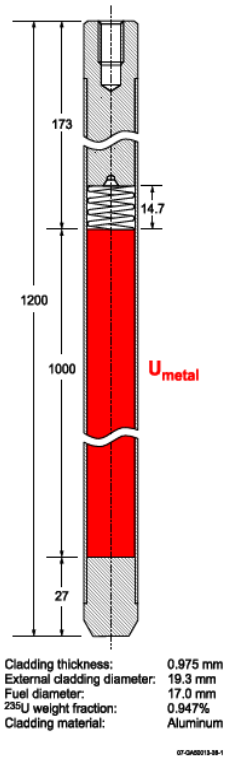

Fig. 4. U_{metal} rods (courtesy of the IRPhe).

During operations, the inverse period (ω_1) can be derived through the measurement of the reactor power P(t) as indicated by formula (1).

2.4. Experimental uncertainties

The uncertainty calculations were performed using the 2D BOXER deterministic code in 15 energy groups for both H_1 (critical level 96.51 cm) and H_4 (water level at 99.51 cm). It should be noted that only the main part of the uncertainty was reported in the benchmark. As a consequence, uncertainties of ^{234}U, ^{236}U contents, fuel impurities, water density, water temperature and impurity content are not given in this paper.

$\rho(H_1) = 0$ and $\rho(H_4) = 129.46$ pcm.

Uncertainties pertaining to the fuel rods were propagated in terms of reactivity and the results are provided in Table 3.

Table 3
Uncertainties pertaining to the fuel rods (IRPhe Handbook).

Parameter	Variation	Δρ (pcm)
Clad thickness (mm)	+0.05	-0.34
Outer clad diameter (mm)	+0.1	+0.26
Fuel diameter UO_2/U_{metal} (mm)	+0.017/+0.02	-0.22
^{235}U enrichment (%)	+0.0007	-0.02
Square pitch (mm)	+0.002	+0.00
Fuel density UO_2/U_{metal} (g/cm^3)	+0.034/+0.044	-0.22

The effects of the inaccuracies of the axial data were evaluated through axial calculations of the central part of CROCUS (i.e., along the UO_2 zone), followed by a calculation of the extrapolated height (based on a cosine fit of the axial power density distribution) and the determination of the axial buckling B_z^2 (IRPhe Handbook).

The propagated uncertainties due to the axial data for cases 1 to 4 are given in **Table 4**.

Table 4
Uncertainties due to grids and plates (IRPhe Handbook).

Parameter	Variation (mm)	Δρ (pcm)
Base plate	+0.1	0
Lower grid	+0.1	0
Lower cadmium plate	+0.05	0
Lower grid	+0.1	-0.03
Upper grid	+0.1	0

Parameter	Variation (mm)	Δρ (pcm)
Upper Cd plate	+0.05	0
Upper grid	+0.1	0
Upper rod parts	+0.5	0

Concerning cases 5 and 6 involving absorbing rods, the propagation of uncertainties due to absorbing rods on reactivity are estimated in **Table 5**.

Table 5
Uncertainties due to absorbing rods (IRPhe Handbook).

Parameter	Poison	Δρ (pcm)
Al clad radius in/out: +0.05 mm	Boron	+2.42
	Erbium	+0.50
Al clad thickness: +0.05 mm	Boron	+0.29
	Erbium	+0.51
Boron density: +0.1%	Boron	+0.07
Er pellet density: +1.0%	Erbium	+1.05
Er pellet diameter: +0.2%	Erbium	+0.41

The uncertainties were calculated separately for each independent parameter. The global uncertainty was then calculated as being the square root of the quadratic sum of each component.

Finally,

$$\Delta\rho(H2) = \pm 0.36\ pcm$$

$$\Delta\rho(H3) = \pm 0.45\ pcm$$

$$\Delta\rho(H4) = \pm 0.53\ pcm$$

$$\Delta\rho(H5) = \pm 2.46\ pcm$$

$$\Delta\rho(H6) = \pm 1.50\ pcm$$

3. Codes and libraries

3.1. Codes

The MORET 5.D.1 (Cochet et al., 2013) Monte Carlo code is used in its continuous energy version using 3D geometry and various nuclear data libraries.

The MCNP5, MCNP6 (Brown et al., 2017) and TRIPOLI-4 (Brun et al., 2015) codes are used as reference routes for a purpose of comparison with the MORET 5.D.1 continuous energy route.

MORET 5.D.1 and MCNP6 models were realized by the authors of this paper. The TRIPOLI-4 results are were taken from published references.

3.2. Nuclear data libraries

The codes and nuclear data libraries are gathered in Table 6.

Table 6
Codes and libraries used for the verification process.

Code	Library
MORET 5.D.1 (Cochet et al. 2015)	JEFF-3.1.1, JEFF-3.3, ENDF/B-VII.0, ENDF/B-VII.1, ENDF/B-VIII.0
MCNP5	ENDF/B-VII.0
MCNP6 (Brown et al. 2017)	ENDF/B-VII.0
TRIPOLI-4 (Brun et al. 2015)	ENDF/B-VII.0

The continuous energy route involves the MORET 5.D.1 code. It solves the transport equation to calculate fluxes and k_{eff} of the 3D configuration. It uses nuclear data processed in the ACE format coming from various libraries.

The MCNP5, MCNP6 and TRIPOLI-4 codes are used to make comparisons with the MORET 5 continuous energy code. All are 3D Monte Carlo codes that solve the neutron transport equation. The MCNP6 and MORET 5 codes use exactly the same nuclear data libraries processed at the ACE format by the same homemade GAIA1.1 processing code (Haeck et al., 2015), based on the 99.259 release of NJOY for the ENDF/B-VII.0 evaluation.

TRIPOLI-4 uses nuclear data of the same evaluation from PENDF files generated by another processing tool.

For MCNP6 results, a comparison was made between results obtained with the ACE files generated by the IRSN GAIA tool but also with the ACE files delivered with the MCNP6 code, allowing an estimate of the processing bias.

4. Theory of kinetics parameters

When considering the population of neutrons and precursors (**Keepin & al, 1965**), two neutron quantities can be singled out: the effective neutron lifetime Λ_{eff} and the effective delayed neutron fraction β_{eff}. They appear in formula (2) and (3).

$$\frac{dN}{dt} = \frac{\rho-\beta_{eff}}{\Lambda_{eff}} N(t) + \sum_{i=1}^{p} \lambda_i C_i(t) \quad (2)$$

$$\frac{dC_i}{dt} = \beta_i \frac{k_{eff}}{l(t)} N(t) - \lambda_i C_i(t) \quad (3)$$

Where ρ is the reactivity,

N(t) is the neutron population,
C_i is the delayed neutron precursor population of type i,
β_i is the effective fraction of precursor family i,
λ_i is the corresponding decay constant for precursor family I,
β_{eff} is the effective delayed neutron fraction,
Λ_{eff} is the neutron generation time,
k_{eff} is the effective multiplication factor,
p is the number of precursors for delayed neutrons,
l(t) is the prompt neutron lifetime.

4.1. Effective neutron lifetime Λ_{eff}

The effective neutron lifetime is the mean time between the birth and the death of a neutron weighted by its contribution to the chain reaction. It is defined by formula (4):

$$\Lambda_{eff} = \frac{<\phi^+, V^{-1}\phi>}{<\phi^+, F\phi>} \quad (4)$$

Where F is the operator for the total fission,

ϕ is the angular flux,

V is the velocity,

ϕ^+ is the adjoint flux, solution of the adjoint Boltzmann equation and representing for this work the importance of a neutron in the Monte Carlo simulation (this quantity is not specific of Monte Carlo simulations).

As a consequence, ϕ^+ is a key parameter to assess the effective neutron lifetime. It is directly linked to the adjoint source Q^+ defined in formula (5).

$$Q^+(r) = \int \frac{1}{4\pi} \chi(E')dE' \int \phi^+(r, E', \Omega')d\Omega' \quad (5)$$

This integral can be evaluated with Monte Carlo methods by sampling the neutron birth spectrum and direction according to an isotropic law. If we write the random vector $\xi_l(E_l,\Omega_l)$ with E_l being the sampled energy and Ω_l the sampled direction, the formula can be moved to equation (6), where L is the number of independent realizations of the estimator Q^+ at the point r.

$$Q^+(r) = \frac{1}{L}\sum_l \phi^+(r, \xi_l) \quad (6)$$

The importance function ϕ^+ has to be estimated. The work of H. Hurwitz (**Radkowsky et al., 1964**) allows approximating this function by the Iterative Fission Probability (IFP) model. Some details about the implementation of the methodology in the Monte Carlo code MORET 5.D.1 are provided in (**Jinaphanh et al., 2017**).

4.2. Effective delayed neutron fraction β_{eff}

The effective delayed neutron fraction β_{eff} is a quantity related to the production of neutrons that are emitted with a delay after fission due to a β^- decay of fission fragments which is followed by a neutron emission (it is the result of the de-excitation energy of a highly excited neutron-rich nuclei obtained by β-decay). It is the ratio between the delayed neutron production rate and the total (delayed and prompt) neutron production rate, those two rates being weighted by the importance function (formula (7) to formula (9)).

$$\beta_{eff} = \frac{P_{effd}}{P_{eff}} \quad (7)$$

$$P_{eff} = <\phi^+, F\phi> = \int \phi^+(r, E, \Omega)\nu_t\chi_t(E, E')\Sigma_f\phi(r, E', \Omega')dE'd\Omega'dEd\Omega dr \quad (8)$$

$$P_{effd} = <\phi^+, B\phi> = \int \phi^+(r, E, \Omega)\nu_d\chi_d(E, E')\Sigma_f\phi(r, E', \Omega')dE'd\Omega'dEd\Omega dr \quad (9)$$

Where B is the operator for the delayed neutron part of the fission source,

χ_t (E,E') is the total fission spectrum, ν_t is the total number of neutrons per fission, χ_d (E,E') is the delayed neutron fission spectrum, ν_d is the expected number of delayed neutrons per fission.

5. Methodology for verification

The verification of the aforementioned codes is done through the comparison of the calculated k_{eff} with the MORET 5 code and the calculated k_{eff} with another code (TRIPOLI-4, MCNP5, MCNP6). If the discrepancy between these two k_{eff} values is lower than the combined standard deviation (see equation 10) of the two Monte Carlo standard deviations (σ_{MC}) (see equation (10)), then no bias can be highlighted.

$$\sigma_{combined} = \sqrt{\sigma_{MC1}^2 + \sigma_{MC2}^2} \qquad (10)$$

Various libraries are tested for continuous energy codes to assess the impact of nuclear data.

When it is not stated, the Monte Carlo standard deviation is equal to 10 pcm, which leads to a combined standard deviation at 3σ of about 45 pcm.

Moreover, whenever the reactivity worth of an element replaced with another is tested, the calculated k_{eff} corresponds to the k_{eff} with the replaced element minus the k_{eff} of the reference case.

In a second step, the results (k_{eff}, reactivity effects, kinetics parameters) of the MORET 5, MCNP5, TRIPOLI-4 and MCNP6 continuous energy codes are compared to one another using the same libraries. It allows evaluating biases due to the implementation of the physical models in the MORET 5 codes.

6. Verification of results

When it is not specified, the MORET 5 calculations are run using the 5.D.1 release of the MORET code, with the probability tables activated in the unresolved energy range of cross sections. Moreover, S(α,β) treatment is used to deal with the hydrogen bindings in water in the low energy range.
MORET 5 results are compared in this section with MCNP5, MCNP6 and TRIPOLI 4 results. The MORET 5 and MCNP6 models were developed independently at IRSN; the MCNP6 results use either ACE files processed by the IRSN GAIA1.1 tool or ACE files delivered with the code. The TRIPOLI-4 models were performed by CEA (Zoia et al., 2016)

6.1. k_{eff} results with continuous energy codes

Six configurations are studied in this section. Only the first one (H1) is critical, the other ones being slightly supercritical.

The k_{eff} results using the ENDF/B-VII.0 based library are reported in **Table 7**. This library is chosen as a reference since TRIPOLI and MCNP calculations use it. It should be noted that a Monte Carlo standard deviation of calculations of 0.00005 was targeted. A total of 38720 neutrons per batch and 4371 batches were necessary to reach good convergence. Statistical tests (Chi2 and Lilliefors) can ascertain this good convergence. The convergence curve for case H1 is reported on Fig. 5. After 1500 batches, the convergence on k_{eff} is obtained. The same type of convergence was obtained for other cases.

The same ACE files are used for the nuclear data in the MORET 5 and MCNP6 codes. TRIPOLI-4 and MCNP5 nuclear data are processed independently. MORET 5, MCNP5 and TRIPOLI-4 results are quite consistent. Moreover, a good agreement is obtained between MCNP5 and MCNP6 using the ACE files delivered with the code.

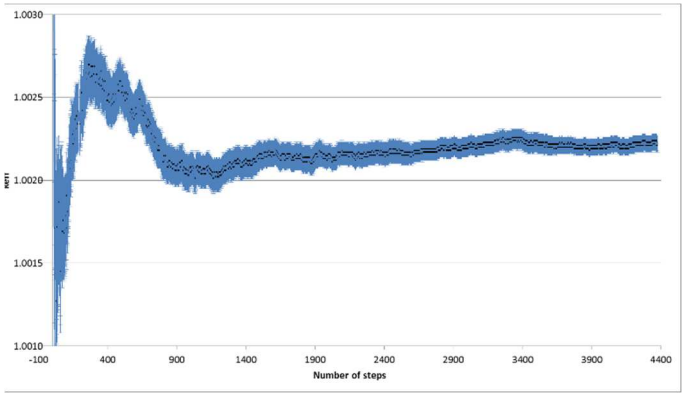

Fig. 5. Convergence of k_{eff} values.

One can derive the reactivity effects corresponding to the supercritical states applying below formula.
$\rho_k = 10^5 \left(\frac{1}{k_{eff}^{crit}} - \frac{1}{k_{eff}^{*}}\right)$, where "crit" corresponds with the critical state and "*" with the supercritical states. A quite good agreement within the uncertainty margins is obtained between the results from MCNP5, MCNP6 (ACE delivered) TRIPOLI-4

(Zoia et al., 2016). However, discrepancies associated with the processing can be identified when looking at the MCNP6 results using the ACE files processed by IRSN. These discrepancies are not surprising; they have already been identified on other benchmarks and suggest that the processing can be source of significant discrepancies on the k_{eff} results.

One can also notice that k_{eff} obtained with MORET 5 are quite consistent with k_{eff} obtained with MCNP6 (IRSN processing), validating the implementation of physical models in MORET 5[c].

Small discrepancies appear between reactivity results, the difference between codes being within the combined 3σ of the Monte Carlo simulation. However, a quite good agreement is obtained between the reactivity given by MCNP5, MCNP6 and TRIPOLI-4. The MORET 5 results, even if in the 3σ uncertainty margins seem to slightly overestimate the value for some cases.

Table 7

keff ± σ_{MC} results with MORET 5, TRIPOLI-4 and MCNP6 codes**.**

Case	MORET 5.D.1	MCNP5 (Zoia et al., 2016)	MCNP6 ACE files delivered	MCNP6 IRSN processing	TRIPOLI-4 (Zoia et al., 2016)
		ENDF/B-VII.0			
H1	1.00289±0.00005	1.00253±0.000012	1.00263±0.00004	1.00294±0.00004	1.00249±0.00002
H2	1.00368±0.00004	1.00341±0.000009	1.00336±0.00004	1.00379±0.00004	1.00335±0.00002
H3	1.00396±0.00005	1.00363±0.000014	1.00366±0.00004	1.00409±0.00004	1.00360±0.00002
H4	1.00410±0.00004	1.00383±0.00002	1.00377±0.00004	1.00433±0.00004	1.00383±0.00002
B	1.00378±0.00005	1.00330±0.000016	1.00321±0.00004	1.00369±0.00003	1.00329±0.00002
Er	1.00447±0.00005	1.00403±0.000021	1.00406±0.00004	1.00446±0.00004	1.00400±0.00002

Table 8

Reactivity results (in pcm) with MORET 5, TRIPOLI-4, MCNP5 and MCNP6 codes (σ_{MC} in pcm) – For boron and erbium cases, the calculation is performed with absorber rods extracted.

Case	MORET 5.D.1	MCNP5 (Zoia et al, 2016)	MCNP6 ACE files delivered	MCNP6 IRSN processing	TRIPOLI-4 (Zoia et al., 2016)
		ENDF/B-VII.0			
H2	78±5	87.5±1.5	73±6	84±6	85.6±3.3
H3	106±5	108.7±1.9	102±6	114±6	110.4±3.3

[c] It should be noticed that the MORET 5 model does not include the 0.025 cm cadmium sheet of the lower grid plate; indeed, an issue with the simulation has been identified. However, it has been verified with MCNP calculations that the worth of this Cd sheet was negligible. The removal of this sheet corrects the bias introduced by the simulation issue.

H4	120±5	128.2±2.3	113±6	138±6	133.0±3.3
B	88±5	82.3±2.5	58±6	75±6	80.8±3.3
Er	157±5	158.8±2.2	142±6	151±6	163.7±3.3

Table 9.a

kinetics parameters – comparison with MCNP6 and TRIPOLI-4.

Parameter	Case	MORET 5.D.1	MCNP5 (Zoia et al., 2016)	MCNP6 (ACE delivered)	MCNP6 (IRSN processing)	TRIPOLI-4 (Zoia et al., 2016)
		ENDF/B-VII.0				
β_{eff} (pcm)	H1	731.15±4.09	737.4±2.7	745±10	728±10	738.3±0.96
Λ_{eff} (μs)		48.05±0.026	47.49±0.02	47.32±0.07	47.48±0.06	47.52±0.006
β_{eff} (pcm)	H2	732.24±3.99	738.3±2.7	744±11	734±10	737.2±0.96
Λ_{eff} (μs)		48.02±0.026	47.43±0.02	47.46±0.06	47.46±0.06	47.50±0.006
β_{eff} (pcm)	H3	730.81±3.98	742.0±2.9	741±11	736±10	736.2±0.96
Λ_{eff} (μs)		48.06±0.026	47.43±0.02	47.43±0.06	47.44±0.06	47.47±0.006
β_{eff} (pcm)	H4	732.59±3.88	741.4±2.9	748±11	749±10	737.2±0.96
Λ_{eff} (μs)		47.99±0.0025	47.43±0.02	47.52±0.06	47.42±0.06	47.47±0.006
β_{eff} (pcm)	B	737.04±3.91	736.4±2.5	757±11	730±10	737.5±0.96
Λ_{eff} (μs)		48.09±0.025	47.52±0.02	47.65±0.06	47.60±0.06	47.62±0.006
β_{eff} (pcm)	Er	726.71±3.94	739.4±3.0	732±11	738±10	734.9±0.95
Λ_{eff} (μs)		48.13±0.026	47.53±0.02	47.55±0.06	47.51±0.06	47.57±0.006

Table 10

kinetics parameters – comparison with MCNP5 taken as a reference R1 = (Code – MCNP5)/ MCNP5 in %.

Parameter	Case	MORET 5.D.1 vs MCNP5	MCNP6 (ACE delivered) vs MCNP5	MCNP6 (IRSN processing) vs MCNP5	TRIPOLI-4 (Zoia et al., 2016) vs MCNP5
		ENDF/B-VII.0			
β_{eff} (pcm)	H1	-0.85	-1.03	-1.55	0.12
Λ_{eff} (μs)		1.18	-0.36	0.19	0.06
β_{eff} (pcm)	H2	-0.82	0.77	2.13	-0.15
Λ_{eff} (μs)		1.24	0.06	-0.02	0.15
β_{eff} (pcm)	H3	-1.51	-0.13	-2.02	-0.78
Λ_{eff} (μs)		1.33	0.00	0.15	0.08
β_{eff} (pcm)	H4	-1.19	0.89	-1.13	-0.57
Λ_{eff} (μs)		1.18	0.19	0.08	0.08
β_{eff} (pcm)	B	0.09	2.80	-1.68	0.15
Λ_{eff} (μs)		1.20	0.27	0.17	0.21
β_{eff} (pcm)	Er	-1.72	-1.00	0.49	-0.61
Λ_{eff} (μs)		1.26	0.04	-0.08	0.08

Table 11
Variation of kinetics parameters values for CROCUS benchmarks versus nuclear data evaluation – MORET 5 code.

Parameter	Case	Kinetic parameter (library effect)			
		ENDF/B-VII.1 vs ENDF/B-VII.0 (%)	**ENDF/B-VIII.0 vs ENDF/B-VII.0 (%)**	**JEFF-3.1.1 vs ENDF/B-VII.0 (%)**	**JEFF-3.3 vs ENDF/B-VII.0 (%)**
β_{eff} (pcm)	H1	0.12	0.34	3.16	3.23
Λ_{eff} (μs)		0.00	-0.62	0.12	-0.48
β_{eff} (pcm)	H2	0.27	0.55	3.18	3.54
Λ_{eff} (μs)		0.00	-0.59	0.14	-0.48
β_{eff} (pcm)	H3	0.07	0.43	3.05	3.28
Λ_{eff} (μs)		-0.02	-0.67	0.10	-0.53
β_{eff} (pcm)	H4	0.03	0.17	3.23	3.01
Λ_{eff} (μs)		0.02	-0.60	0.14	-0.48
β_{eff} (pcm)	B	-0.08	0.14	2.80	2.86
Λ_{eff} (μs)		0.00	-0.59	0.18	-0.46
β_{eff} (pcm)	Er	-0.15	0.39	2.62	2.82
Λ_{eff} (μs)		0.12	0.34	3.16	3.23

Table 7

$k_{eff} \pm \sigma_{MC}$ results with MORET 5, TRIPOLI-4 and MCNP6 codes**.**

Case	MORET 5.D.1	MCNP5 (Zoia et al., 2016)	MCNP6 ACE files delivered	MCNP6 IRSN processing	TRIPOLI-4 (Zoia et al., 2016)
		ENDF/B-VII.0			
H1	1.00289±0.00005	1.00253±0.000012	1.00263±0.00004	1.00294±0.00004	1.00249±0.00002
H2	1.00368±0.00004	1.00341±0.000009	1.00336±0.00004	1.00379±0.00004	1.00335±0.00002
H3	1.00396±0.00005	1.00363±0.000014	1.00366±0.00004	1.00409±0.00004	1.00360±0.00002
H4	1.00410±0.00004	1.00383±0.00002	1.00377±0.00004	1.00433±0.00004	1.00383±0.00002
B	1.00378±0.00005	1.00330±0.000016	1.00321±0.00004	1.00369±0.00003	1.00329±0.00002
Er	1.00447±0.00005	1.00403±0.000021	1.00406±0.00004	1.00446±0.00004	1.00400±0.00002

Table 8

Reactivity results (in pcm) with MORET 5, TRIPOLI-4, MCNP5 and MCNP6 codes (σ_{MC} in pcm) – For boron and erbium cases, the calculation is performed with absorber rods extracted.

Case	MORET 5.D.1	MCNP5 (Zoia et al, 2016)	MCNP6 ACE files delivered	MCNP6 IRSN processing	TRIPOLI-4 (Zoia et al., 2016)
		ENDF/B-VII.0			
H2	78±5	87.5±1.5	73±6	84±6	85.6±3.3
H3	106±5	108.7±1.9	102±6	114±6	110.4±3.3
H4	120±5	128.2±2.3	113±6	138±6	133.0±3.3
B	88±5	82.3±2.5	58±6	75±6	80.8±3.3
Er	157±5	158.8±2.2	142±6	151±6	163.7±3.3

Table 9.a

kinetics parameters – comparison with MCNP6 and TRIPOLI-4.

Parameter	Case	MORET 5.D.1	MCNP5 (Zoia et al., 2016)	MCNP6 (ACE delivered)	MCNP6 (IRSN processing)	TRIPOLI-4 (Zoia et al., 2016)
		ENDF/B-VII.0				
β_{eff} (pcm)	H1	731.15±4.09	737.4±2.7	745±10	728±10	738.3±0.96
Λ_{eff} (μs)	H1	48.05±0.026	47.49±0.02	47.32±0.07	47.48±0.06	47.52±0.006
β_{eff} (pcm)	H2	732.24±3.99	738.3±2.7	744±11	734±10	737.2±0.96
Λ_{eff} (μs)	H2	48.02±0.026	47.43±0.02	47.46±0.06	47.46±0.06	47.50±0.006
β_{eff} (pcm)	H3	730.81±3.98	742.0±2.9	741±11	736±10	736.2±0.96
Λ_{eff} (μs)	H3	48.06±0.026	47.43±0.02	47.43±0.06	47.44±0.06	47.47±0.006
β_{eff} (pcm)	H4	732.59±3.88	741.4±2.9	748±11	749±10	737.2±0.96
Λ_{eff} (μs)	H4	47.99±0.0025	47.43±0.02	47.52±0.06	47.42±0.06	47.47±0.006
β_{eff} (pcm)	B	737.04±3.91	736.4±2.5	757±11	730±10	737.5±0.96
Λ_{eff} (μs)	B	48.09±0.025	47.52±0.02	47.65±0.06	47.60±0.06	47.62±0.006
β_{eff} (pcm)	Er	726.71±3.94	739.4±3.0	732±11	738±10	734.9±0.95
Λ_{eff} (μs)	Er	48.13±0.026	47.53±0.02	47.55±0.06	47.51±0.06	47.57±0.006

Table 10

kinetics parameters – comparison with MCNP5 taken as a reference R_1 = (Code – MCNP5)/ MCNP5 in %.

Parameter	Case	MORET 5.D.1 vs MCNP5	MCNP6 (ACE delivered) vs MCNP5	MCNP6 (IRSN processing) vs MCNP5	TRIPOLI-4 (Zoia et al., 2016) vs MCNP5
		ENDF/B-VII.0			
β_{eff} (pcm)	H1	-0.85	-1.03	-1.55	0.12
Λ_{eff} (μs)	H1	1.18	-0.36	0.19	0.06
β_{eff} (pcm)	H2	-0.82	0.77	2.13	-0.15
Λ_{eff} (μs)	H2	1.24	0.06	-0.02	0.15
β_{eff} (pcm)	H3	-1.51	-0.13	-2.02	-0.78
Λ_{eff} (μs)	H3	1.33	0.00	0.15	0.08
β_{eff} (pcm)	H4	-1.19	0.89	-1.13	-0.57
Λ_{eff} (μs)	H4	1.18	0.19	0.08	0.08
β_{eff} (pcm)	B	0.09	2.80	-1.68	0.15
Λ_{eff} (μs)	B	1.20	0.27	0.17	0.21
β_{eff} (pcm)	Er	-1.72	-1.00	0.49	-0.61
Λ_{eff} (μs)	Er	1.26	0.04	-0.08	0.08

Table 11
Variation of kinetics parameters values for CROCUS benchmarks versus nuclear data evaluation – MORET 5 code.

Parameter	Case	Kinetic parameter (library effect)			
		ENDF/B-VII.1 vs ENDF/B-VII.0 (%)	**ENDF/B-VIII.0 vs ENDF/B-VII.0 (%)**	**JEFF-3.1.1 vs ENDF/B-VII.0 (%)**	**JEFF-3.3 vs ENDF/B-VII.0 (%)**
β_{eff} (pcm)	H1	0.12	0.34	3.16	3.23
Λ_{eff} (μs)		0.00	-0.62	0.12	-0.48
β_{eff} (pcm)	H2	0.27	0.55	3.18	3.54
Λ_{eff} (μs)		0.00	-0.59	0.14	-0.48
β_{eff} (pcm)	H3	0.07	0.43	3.05	3.28
Λ_{eff} (μs)		-0.02	-0.67	0.10	-0.53
β_{eff} (pcm)	H4	0.03	0.17	3.23	3.01
Λ_{eff} (μs)		0.02	-0.60	0.14	-0.48
β_{eff} (pcm)	B	-0.08	0.14	2.80	2.86
Λ_{eff} (μs)		0.00	-0.59	0.18	-0.46
β_{eff} (pcm)	Er	-0.15	0.39	2.62	2.82
Λ_{eff} (μs)		0.12	0.34	3.16	3.23

6.2. Reactivity worth of absorbing rods

The reactivity worth of absorbing rods is obtained by comparison between k_{eff} with rods fully inserted and k_{eff} with rods extracted from the core. It is reported in **Table 12**. No significant discrepancy between reactivity worth from MORET 5.D.1 and MCNP6 can be observed.

Table 12
Reactivity worth of boron and erbium in absorbing rods.

Case	MORET 5.D.1	MCNP6 (Processing IRSN)
	ENDF/B-VII.0	
B - inserted	1.00275 ± 0.00007	1.00284±0.00004
Er - inserted	1.00278 ± 0.00007	1.00277±0.00004
B - extracted	1.00378 ± 0.00005	1.00369±0.00004
Er - extracted	1.00447 ± 0.00005	1.00446±0.00004
B – Δk_{eff} (pcm)	-103 ± 9	-85 ± 4
Er – Δk_{eff} (pcm)	-169 ± 9	-169 ± 5

6.3. Effect of nuclear data

6.3.1. Multiplication factor

Various nuclear data evaluations (JEFF-3.1.1, JEFF-3.3, ENDF/B-VII.0, ENDF/B-VII.1 and ENDF/B-VIII.0) were tested with the MORET 5.D.1 Monte Carlo code to see if an impact of nuclear data could be isolated for k_{eff} and kinetics parameters assessment (see **Table 13**). Regarding k_{eff}, no significant discrepancy between libraries can be pointed out. A similar conclusion was drawn in the paper by Zoia et al. (2016), where results were consistent for all libraries, except for JENDL-40 for which a small 40-50 pcm underestimation due to the hydrogen bound S(α,β) temperature could be highlighted.

6.3.2. Kinetics parameters

The effective delayed neutron fraction β_{eff} as well as the effective mean generation time Λ_{eff} are calculated using the Monte Carlo MORET 5.D.1 and MCNP6 codes. In the MORET 5 simulation, various estimators are used to evaluate the two parameters; however, it was chosen to keep only the results from the adjoint flux estimator. Indeed, this new option in the MORET 5 code gives a better assessment of the adjoint flux as it was done in the previous releases. The neutrons produced by fissions are accounted for during several generations and not only one.

Results are gathered in **Table 10**Error! Reference source not found. and compared with the MCNP and TRIPOLI-4 codes. One can notice that the two coefficients do not depend strongly on the experiment number.

A comparison is performed based on the following coefficient: R_1 = (code result – MCNP5 result)/MCNP5 result.

No significant discrepancy on β_{eff} between codes can be observed, the R_1 coefficient remaining lower than 1.5 %. Very good agreement is observed between MCNP6, MCNP5 and TRIPOLI-4 results for the Λ_{eff}. However, a larger discrepancy up to 1.5 % is observed with MORET. The reason for that discrepancy is still under investigation but the fact that MORET uses the same neutron spectrum for prompt and delayed neutrons could explain it. This discrepancy can exceed the 3σ of Monte Carlo standard deviation but the estimated standard deviation of Monte Carlo calculation of Λ_{eff} might be strongly underestimated. Finally, the values obtained with MORET 5 are very close to MCNP and TRIPOLI values.

Additionally, one can notice some discrepancy between the JEFF and ENDF evaluations. All results coming from the JEFF evaluations are consistent with one another; similarly, all results produced with the various releases of the ENDF evaluations are consistent with one another. This tendency was already identified in the paper by Zoia et al. (2016), especially for β_{eff}. JEFF-3 results were systematically higher than ENDF results. A calculation was performed replacing only ^{235}U, only ^{238}U and ^{235}U+^{238}U ENDF/B-VII.0 nuclear data by the JEFF-3.3 ones. We observe that the discrepancy is mainly due to ^{235}U. This discrepancy could be explained by the fission spectrum of ^{235}U differing between the two evaluations.

Table 13
Δk_{eff} for CROCUS benchmarks versus nuclear data evaluation – MORET 5 code.

Case	ΔK_{eff} (library effect) (σ_{MC} = 0.00005) in pcm			
	B-VII.1-B-VII.0	B-VIII.0-B-VII.0	JEFF-3.1.1-B-VII.0	JEFF-3.3-B-VII.0
H1	0	-19	5	55
H2	0	-41	-2	33
H3	-6	-15	0	47
H4	-4	-32	-4	39
B	-22	-27	-2	19
Er	-5	-33	-13	27

6.4. Spectral indices

Spectral indices such as the flux on the whole geometry and ^{235}U fission rate as well as ^{238}U capture rate calculated by the MORET 5.D.1 code are reproduced in Fig. 6 to Fig. 8.
The CROCUS reactor being a light water reactor it is logical to find that neutrons are captured in the epithermal and thermal energy ranges and undergoing fissions in the thermal energy range. The flux profile is typical of that kind of reactors.

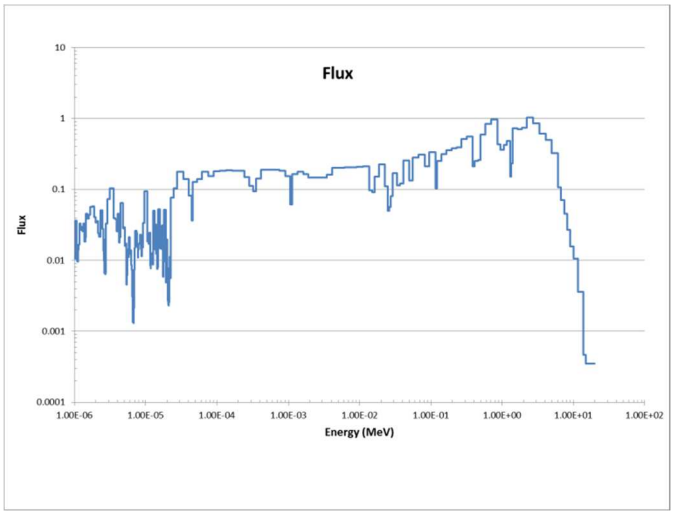

Fig. 6. Flux on the whole geometry.

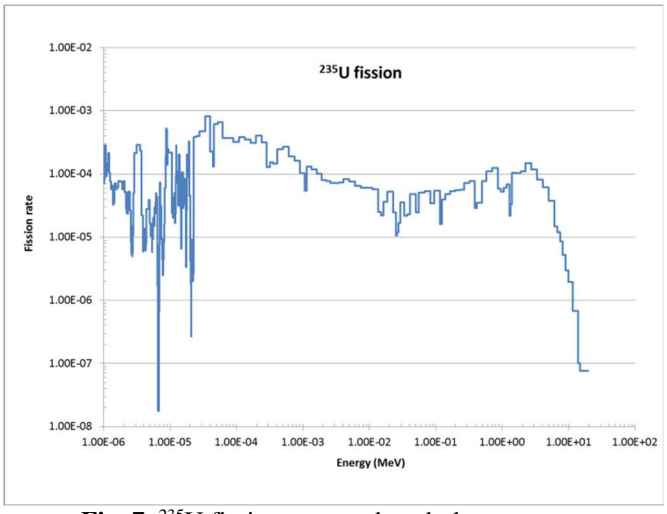

Fig. 7. ^{235}U fission rate on the whole geometry.

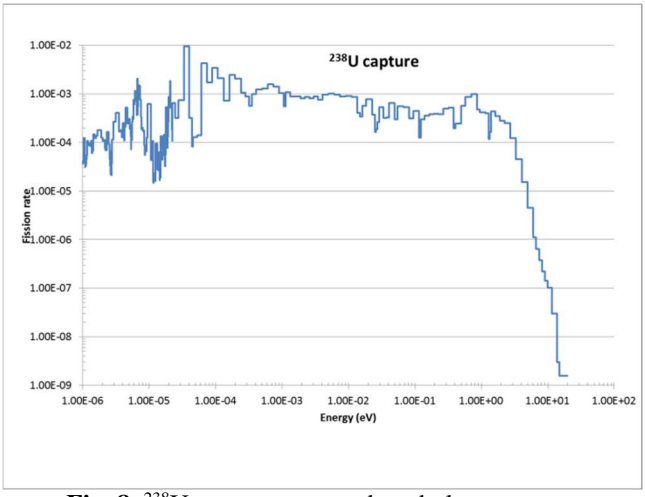

Fig. 8. ^{238}U capture rate on the whole geometry.

6.5. Sensitivity to nuclear data

The 5.D.1 release of the MORET 5 code offers the opportunity to calculate sensitivity coefficients of k_{eff} to the main reactions (cross sections and angular distributions). Such calculations are based on the Iterated Fission Probability technique (IFP) (Jinaphanh et al., 2017) also implemented in the SCALE (Rearden et al., 2004) and MCNP6.2 (Kiedrowski et al., 2013) codes. The method used for implementation is the differential operator method. In this method, the estimation of the fission source derivatives is replaced by an estimation of the adjoint flux. For the main reactions (^{235}U fission, ^{235}U capture, ^{238}U capture, ^{1}H capture…), the sensitivity profiles calculated using the MORET 5.D.1 and MCNP6.2 Monte Carlo codes with the ENDF/B-VII.0 nuclear data library are plotted against energy (Fig. 9. to Fig 12.). The ratio between the results provided by the two codes are reported in purple. It appears that the ratios differ from 1 mainly for energy regions where the sensitivity is quite negligible and that the discrepancies are larger for the sensitivity to ^{238}U capture and ^{1}H capture cross sections.

Table 14
Discrepancy on integral sensitivity coefficients between MORET 5 (M5) and MCNP6.

Reaction	Integral sensitivity MORET 5.D.1	Integral sensitivity MCNP6.2	Difference M5/MCNP6 (%)
^{235}U fission	4.077E-01 ± 1.3E-04	4.019E-01 ± 1.3E-04	+1.44
^{235}U capture	-9.709E-02 ± 2.4E-05	-9.844E-02 ± 2.4E-05	-1.37
^{238}U capture	-2.450E-01 ± 6.2E-05	-2.418E-01 ± 6.2E-05	+1.32
^{1}H capture	-1.660E-01 ±4.9E-05	-1.639E-01 ±4.9E-05	+1.28

One can notice, as it is the case for reactor experiments, a sensitivity of k_{eff} to the fission of ^{235}U, to the capture of ^{238}U, and to the capture of ^{1}H in water. These sensitivity profiles could then be used in the MACSENS tool (**Jinaphanh et al., 2017**) to assess the bias and uncertainty due to nuclear data through a GLLSM. Having experiments that are uncorrelated with existing ones and with well-established experimental uncertainties allows having confidence in the calculated bias and associated uncertainty.

The discrepancy between MORET 5.D.1 and MCNP6.2 integral sensitivities to the main reactions (Table 14) remain lower than 2 %, which is quite acceptable since the main discrepancies are in the energy region where the sensitivity is low and also since the standard deviation of Monte Carlo calculations is certainly under-estimated. One can therefore conclude to a quite good agreement between the sensitivity coefficients from MORET 5.D.1 or MCNP6.2, even if the bias with MCNP values exceeds the 3σ standard deviation. It therefore allows verification of the MORET 5.D.1 code.

The discrepancy between integral sensitivity coefficients is reported in **Table 13**.

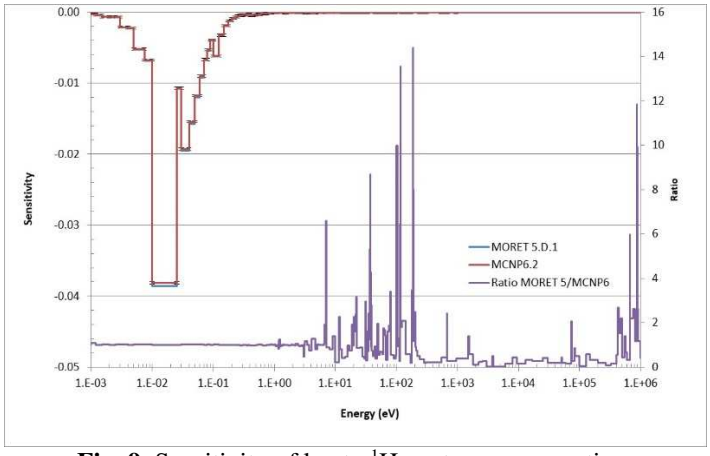

Fig. 9. Sensitivity of k_{eff} to ^{1}H capture cross section.

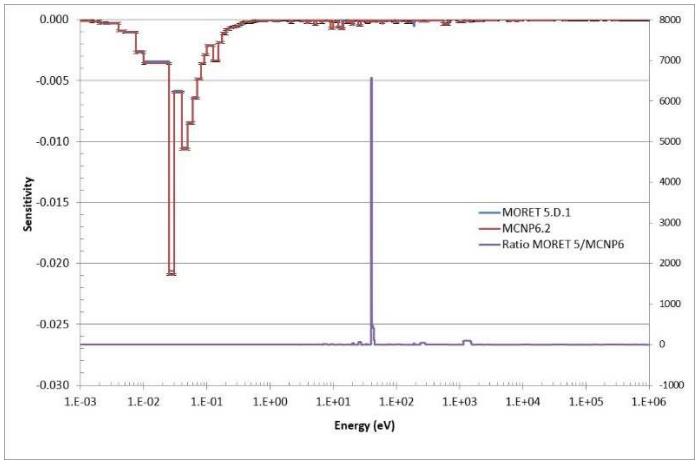

Fig. 10. Sensitivity of k_{eff} to ^{235}U capture cross section.

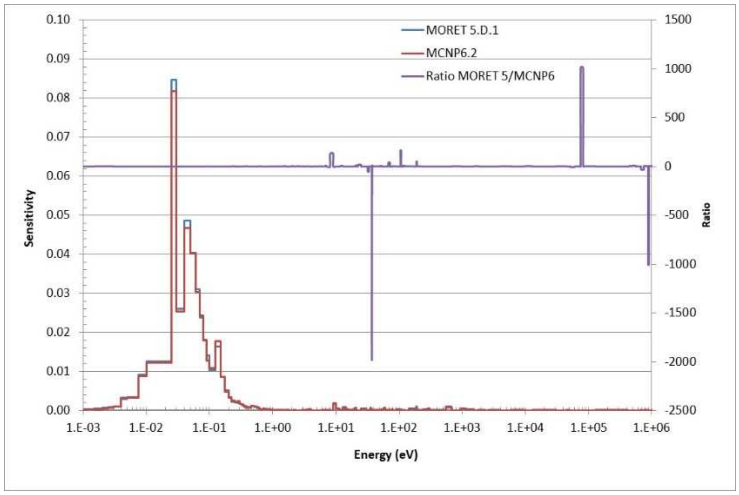

Fig. 11. Sensitivity of k_{eff} to ^{235}U fission,

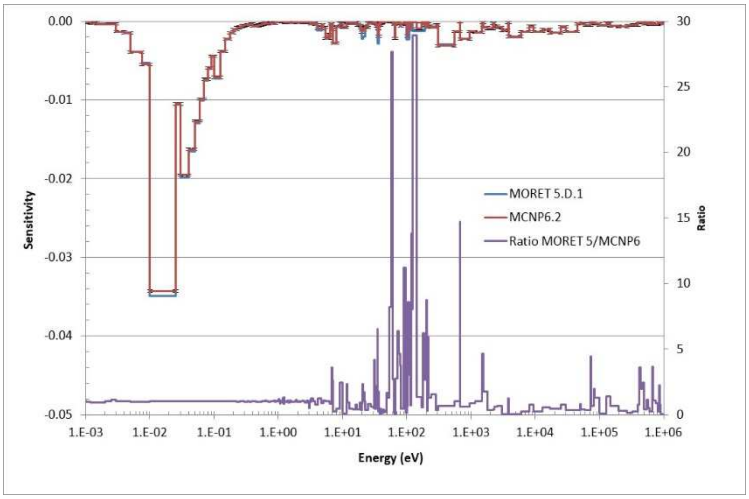

Fig. 12. Sensitivity of k_{eff} to ^{238}U capture cross sections.

7. Conclusion

The purpose of the present paper was to make a verification of physical quantities (k_{eff}, sensitivity coefficients, kinetics parameters) of the MORET 5.D.1 code developed at IRSN on criticality and reactor physics applications. A database of more than 1400 benchmark experiments is already available for criticality safety application. However, the number of cases is far more restricted regarding reactor physics applications. To achieve the goal of verification for reactor physics applications, the CROCUS benchmark was selected as being representative of light water reactors and relatively easy to model.

Several capabilities implemented in the MORET 5.D.1 code were tested using various nuclear data libraries (JEFF-3.1.1, JEFF-3.3, ENDF/B-VII.0, ENDF/B-VII.1 and ENDF/B-VIII.0):

- The calculation of kinetics parameters,
- The sensitivity of k_{eff} to nuclear data (cross sections),
- The production of reaction rates.

When comparing k_{eff} and reactivity results between the MORET 5, MCNP5, TRIPOLI-4 and MCNP6 Monte Carlo codes using the same nuclear data libraries, no significant discrepancy can be pointed out, except when the processing of nuclear data differs.

Another result of the paper is that the effect of the nuclear data library is insignificant regarding k_{eff}, which is not the case for kinetics parameters. Indeed, results from the JEFF libraries are consistent with one another, as is the case for ENDF libraries.

Finally, regarding the calculation of sensitivity coefficients, a quite good agreement is obtained between sensitivity coefficients generated using the MORET 5.D.1 and the MCNP6.2 codes. It therefore contributes to the verification of the sensitivity capability development in the MORET 5.D.1 code.

References

B. Cochet, L. Heulers, A. Jinaphanh, O. Jacquet, “Capabilities overview of the MORET 5 Monte Carlo code”, Annals of Nuclear Energy, p:82-74 · August 2015

J.M. Gomit, I. Duhamel, Y. Richet, A. Entringer, C. Magnaud, F. Malouch, C. Carmouze, « CRISTAL V2: New Package for Criticality Calculations », NCSD 2017, 10-15 sept, Carlsbad,

R. Sanchez, M. Zmijarevic, E. Coste-delclaux, S. Masiello, E. Santandrea et al., APOLLO2 YEAR 2010, Nuclear Engineering and Technology, vol.42, issue.5, 2010,

H. HURWITZ, in Naval Reactor Physics Handbook: Selected Basic Techniques, Vol. 1, p. 864, A. RADKOWSKY, Ed., U.S. Atomic Energy Commission (1964).

A. Jinaphanh, F. Fernex, N. Leclaire, “Uncertainty and Bias quantification with the MACSENS software”, EGUACSA-2017/09, July 2017

L. Leal et al. "Nuclear data and applications at the nuclear safety and radioprotection institute: Analysis, evaluation and application", Annals of Nuclear Energy Volume 134, December 2019, Pages 244-249

A. Jinaphanh, J. Miss, Y. Richet, O. Jacquet, “Calculating the kinetics parameters in the continuous energy Monte Carlo code MORET”, PHYSOR 2010, Pittsburgh, Pennsylvania, USA, May 2010.

NEA/NSC/DOC(2006)01, *IRPhe Handbook (2017)*

F.B. Brown, M.E. Rising, J.A. Alwin, “Release of MCNP6.2 & Whisper-1.1 - Guidance for NCS Users”, ANS 2017 Nuclear Criticality Safety Division Topical Meeting, Carlsbad, NM, LA-UR-17-24260 (2017)

T. Booth, H. Hughes, A. Zukaitis, F. Brown, R. Mosteller M. Boggs, (CCN-12), J. Bull, R. Prael, R. Martz (CCN-7), R. Forster, A. Sood, J. Goorley, J. Sweezy, “MCNP - A General Monte Carlo N-Particle Transport Code, Version 5”, *Los Alamos National Laboratory, (2003)*

B. C. Kiedrowski & F. B. Brown (2013), “Adjoint-Based k-Eigenvalue Sensitivity Coefficients to Nuclear Data Using Continuous-Energy Monte Carlo”, Nuclear Science and Engineering, 174:3, 227-244, DOI: 10.13182/NSE12-46

E. Brun, F. Damian, C.M. Diop, E. Dumonteil, F.X. Hugot, C. Jouanne, Y.K. Lee, F. Malvagi, A. Mazzolo, O. Petit, J.C. Trama, T. Visonneau, A. Zoia, “TRIPOLI-4®, CEA, EDF and AREVA reference Monte Carlo code”, Annals of Nuclear Energy, Volume 82, August 2015, Pages 151-160

W. Haeck, “GAIA User’s Manual - Version 1.0.0”, IRSN Report PSN-EXP/SNC/2015-165, Institut de Radioprotection et de Sûreté Nucléaire, France (2015)

A. Radkowsky, “Naval Reactor Physics Handbook”, vol. 1, Naval reactors, U.S. Atomic Energy Commission (1964),

A. Jinaphanh, N. Leclaire, B. Cochet, “Continuous energy sensitivity coefficients in the MORET code”, Nuclear Science & Engineering, p: 53-68, 2017

A. Zoia, Y. Nauchi, E. Brun, C. Jouanne, “Monte Carlo analysis of the CROCUS benchmark on kinetics parameters calculation”, Annals of Nuclear Energy 96 (2016), p: 377-388, 2016

B.T. Rearden, “Perturbation theory eigenvalue sensitivity analysis with Monte Carlo techniques”, Nuclear Science & Engineering, p:367-382, volume 146, Number 3, March 2004.

G. R. Keepin, 1965. “Physics of Nuclear Kinetics”. Chapter 7: “Asymptotic Period-Reactivity Relations”, p.187. Addison Wesley Publishing Company (1965).

Acknowledgements

The authors would like to thank Valentin Jouault, subcontractor from the URANUS company, and Mariya Brovchenko from IRSN for their support in the modelling of the MCNP configurations and the ICSBEP and IRPhe working groups under the auspices of OECD for their involvement in the production of the Criticality and Reactor Physics Handbooks.